Results in Physics 10 (2018) 281–286

Contents lists available at ScienceDirect

Results in Physics

journal homepage: www.elsevier.com/locate/rinp

Structure and transport properties of Tl_2Te_3 single crystals

I.M. Ashraf[a,b], A. Salem[c,*], M.S. Awad Al-Juman[a]

[a] Department of Physics, Faculty of Science, King Khalid University, P.O. Box 9004, Abha, Saudi Arabia
[b] Department of Physics, Faculty of Science, Aswan University, Aswan, Egypt
[c] Solid State Lab., Physics Department, Faculty of Science, South Valley University, Qena, Egypt

ARTICLE INFO

Keywords:
Semiconductors
XRD
SEM
EDAX
Electrical conductivity
Hall effect
Tl_2Te_3 single crystals

ABSTRACT

A special new design from melt based on the Bridgman technique has been applied to prepare Tl_2Te_3 single crystals. The grown crystals were characterized by XRD, SEM, EDAX. The electrical conductivity, Hall effect and thermoelectric power have been performed over the temperature ranges from 93 K to 448 K and 129 K to 468 K respectively. Many physical constant (such as the energy gap, the depth of the impurity level, the Hall coefficient, the conductivity type, the diffusion length, the diffusion coefficient, the scattering mechanism of the charge carriers and their concentrations, the mobility, effective mass, and the lifetime of the majority and minority carriers) have been estimated. The results show that the prepared Tl_2Te_3 single crystals can be used in the fabrication of electronic devices.

Introduction

The chalcogenide compounds formed from elements of the melt T1-Te system have attracted particular interest for their very wide range of applications in different items, such as electronic devices, electronic refrigeration, photovoltaic devices, and optoelectronic devices [1]. Among the III–VI group semiconductor materials, the Tl-Te system has attracted particular interest and has been investigating for its thermoelectric properties [2–7]. In the Tl-Te system, there are four stoichiometric compounds Tl_2Te_3, TlTe, Tl_2Te and Tl_5Te_3 [8]. After the experimental confirmation of the existence of Tl_2Te_3 by Rabenau et al. in 1960 [9], Bhan and Schubert determined the crystal structure in 1970 (Weissenberg records) [10]. Measurements of the galvanomagnetic effects, the thermoelectric, and electrical conductivity were reported on single crystal specimens of Tl_2Te_3 and TlTe or the γ-phase at various temperatures [11]. All crystals were found to be of p-type conductivity. The electrical conductivity, Hall effect, and thermoelectric power (TEP) measurements have been measured over the temperature range (200–492 K) and (163–602 K) of the layered $TlGaSe_2$ crystals by H.T. Shaban [12]. A simple interchange of the Wyckhoff sites of the Tl and the Te atoms under consideration would avoid this short Tl-Te contacts and would principally give the correct structural features. Lippens and Aldon examined the electronic structure of Tl_5Te_3, TlTe, and Tl_2Te_3 [7]. They also suggested this exchange mentioned above reconcile their results with the known semiconducting properties of Tl_2Te_3 (p-type semiconductor, $E_g = 0.68$ eV [13]). The Tl_2Te_3 phase has semiconducting properties with an energy gap of 0.68 ± 0.03 eV [3]. Doert et al. [14] reinvestigated the crystal structure of Tl_2Te_3 to prove the interchange of the atomic positions and to determine the precise interatomic distances. Two different Te-Te distances are found in Tl_2Te_3. One of them is the bonding contact within the linear triatomic units (3.02 A^0). Cruceanu et al. [15] had reported for the first time the interesting results of the electric properties of TI_2Te_3 where – based on electric conductivity and Hall effect measurements at 93 and 293 K – the compound was found to be a semiconductor. To observe its semiconducting behavior Hall-effect and electrical conductivity measurements were performed on Tl_2Te_3 single crystals by S. A. Hussien et al. [16]. The measurements were done in a wide temperature range from 160 to 350 K. As grown Tl_2Te_3 crystals were found to be a p-type semiconductor. Band gap of the sample was found to be 0.7 eV where the depth of the impurity energy level was 0.45 eV. Thermoelectric power (TEP) measurements have been reported by G.A.Gamal et al. [17] in the temperature range from 150 to 480 K. Although [18] the existence of the compound TI_2Te_3 has been proved as early as 1960, its photo absorption and photoelectric properties have not been reported so far. The present study yields appreciable amounts of information about the actual behaviors that are essential to understanding the materials and consequently their practical application.

Experimental

Single crystals of TI_2Te_3 were grown by direct melting of the elements in quartz ampoules. The required material contained in the quartz tubes, of 12.6365 g of pure Thallium (Aldrich Mark)

* Corresponding author.
E-mail address: aasalem@kku.edu.sa (A. Salem).

https://doi.org/10.1016/j.rinp.2018.05.044
Received 10 December 2017; Received in revised form 29 May 2018; Accepted 29 May 2018
Available online 02 June 2018

representing 49.757% of the 999,999% and 12.7599 g of pure Tellurium (Aldrich Mark) representing 50.243% of the 999,999%, were evacuated and sealed. A special new design from melt based on Bridgman technique was used to prepare our samples. To investigate Tl_2Te_3 single crystals, the samples were characterized using Shimadzu X-ray Diffractometer (XRD-6000) with Cu K α irradiation (λ = 1.54187 Å). Scanning Electron Microscope (SEM) for grown Tl_2Te_3 single crystals was used to characterize the surface morphology. The grown crystals were characterized by Energy Dispersive Spectrum (EDS). We used a JSM 6360 LV SEM to study our samples. For studying the Hall effect and electrical conductivity, the samples were cut into rectangular shapes. The sample size was 5.2 × 1.7 × 1.2 mm^3 after the polishing process. in such a way, L of the rectangle sample was three times its width, to prevent problems related to Hall voltage drop. Ag paste contact was used as an ohmic contact. Measurements of electrical conductivity and Hall effect were performed under a vacuum of $\approx 10^{-4}$ Torr. The measurements were made via a compensation method in a specially designed cryostat by conventional DC type measurement system. The designed cryostat offer a wide range of temperatures from 77 to 500 K. For the thermoelectric power (TEP) measurements, the sample was supported vertically by two holders one of which (the lower one) acts as a heat source, while the other serves as a heat sink. The sample was introduced inside a high vacuum tight calorimeter designed especially for this purpose. The sample was insulated from the holders by a thin sheet of mica. The temperature of the crystal was considered to be the average of those at its two ends. To calculate the absolute thermoelectric power of these samples at different temperatures divide the magnitude of the thermo-voltage difference across the crystal by the temperature difference between the hot-end and cold-end. Then the thermoelectric power is the e.m.f. per degree, Centigrade drop between the hot and cold sides.

Results and discussion

Structural properties of Tl_2Te_3 single crystals

The identification of Tl_2Te_3 compounds was carried out via an X-ray. The θ/2θ diffraction spectra for powdered Tl_2Te_3 single crystals shown in Fig. 1. All the major reflections are indexed as (0 0 ℓ) peaks of Tl_2Te_3 phase as compared with the PDF standard card no. 2:23-0928 with no impurities.

The XRD patterns of Tl_2Te_3 are well consistent with the literature data, so it can be said that the pure compounds with no impurities could be obtained. All d-spacings from goniometer XRD analysis were matched with corresponding d-spacings in the JCPDS database available in the Shimadzu LAB-X XRD-6000 diffract meter operating software to determine all phases present.

The mean crystallite size (D) of the particles was calculated from the XRD line-broadening measurement of the Scherrer equation [19]

$$\beta(2\theta) = \frac{0.89\lambda}{D\cos\theta} \quad (1)$$

The average grain size of the samples was estimated as 7.37 μm by using Scherrer's equation, which corresponds well with what we got from the results of scanning electron microscopy (SEM).

Fig. 2 shows what represents a Scanning Electron Microscopy (SEM) images of the micro-crystals of the sample studied. In the first image, Fig. 2(a) shows homogeneous micro-crystal particles having a perfectly crystalline appearance. The Fig. 2(b) shows microcrystals in detail at 1300× amplification. The typical morphology is clearly exhibited in Fig. 2(c) at 3000× amplification.

DC-electrical properties and Hall effect measurements of Tl_2Te_3 single crystals

Electrical properties of a Tl_2Te_3 single crystal have been studied over a wide temperature range extending from 93 K to 448 K. Fig. 3 shows the temperature dependence of electrical conductivity for the single crystal sample of Tl_2Te_3. The curve shows the typical semiconductor behavior. A typical semiconductor behavior curve consists of three major parts.

Starting from the low temperatures, the first part (93–173 K) represents the extrinsic conduction range where the carrier concentration is mainly determined by the number of ionized acceptors. This naturally occurs as a result of the liberation of ionized acceptors and their transition from the impurity level. Accordingly σ increases slowly. In this range the following formula describes the relation between σ and T:

$$\sigma = \sigma_o \exp(-\Delta E_a/2k_BT) \quad (1)$$

where σ_o is pre-exponential factor and K_B is the Boltzmann's constant. From the above relation, we could calculate the impurity ionization energy ΔE_a. It was found to be 0.124 eV. The second region of the curve (173–253 K), represents the transition region where the behavior of σ is governed by the behavior of both the charge carrier concentration and their mobility. In this region, the small increase in the electrical conductivity is due to the increase in the hole concentration. Above 253 K the intrinsic conduction begins (as seen from the figure) where σ increases sharply. This predicts that both electrons and holes contribute in the conduction at this high-temperature range. The following equation is used to estimate the value of the energy gap.

$$\sigma = \sigma_o \exp(-\Delta E_g/2k_BT) \quad (2)$$

The energy gap width ΔE_g could be calculated. It was found to be 0.686 eV.

The importance of the Hall effect is underscored by the need to accurately determine the carrier density, the electrical resistivity, and the mobility of carriers in semiconductors. So the present investigations are extended to cover this unique phenomenon. In the same temperature range (93–448 K) the variation of the Hall coefficient against temperature was examined. In Fig. 4 the curve is divided mainly into:

- low-temperature part (93 up to about 173 K) which represents the case of the extrinsic conduction.
- The high-temperature part which appears between (253–448 K). R_H at room temperature has a value of 3.06 × 10^5 cm^3/C.
- An intermediate region between 173 and 253 K lies between the intrinsic and extrinsic parts, known as the transition part.

This supports the behavior of the three regions observed in the conductivity curves Fig. 3. From the measurement of the Hall coefficient it is evident that the sign of the Hall coefficient of TI_2Te_3 is positive over the entire range of investigation, indicating that the compound is a p-type semiconductor and the major contribution to conductivity by holes which is in reasonable agreement with the results [18,19] obtained by the other author.

Determination of the energy gap and ionization energy from Hall data is possible by plotting the relation between R_H $T^{3/2}$ and 10^3/T as shown in Fig. 5. From the figure, we also distinguished the three the region at the same corresponding temperatures according to the relation:

$$R_HT^{3/2} = c_1\exp(-\Delta E_g/2k_BT) \quad (3)$$

By using the data presented in Fig. 5, we can determine the band gap energy. It was found to be 0.69 eV. The depth of the impurity the level was also computed and it was found to be 0.118 eV. These values are in a good agreement with those obtained from the temperature dependence of electrical conductivity.

The combination of the electrical and Hall measurements in the present investigation was used to study the temperature-dependence of free-charge carrier mobility. Fig. 6 displays the logarithm of Hall mobility μ plotted against LnT and the result is a straight line. The slope of this straight line plot is then used to calculate the exponent. From the

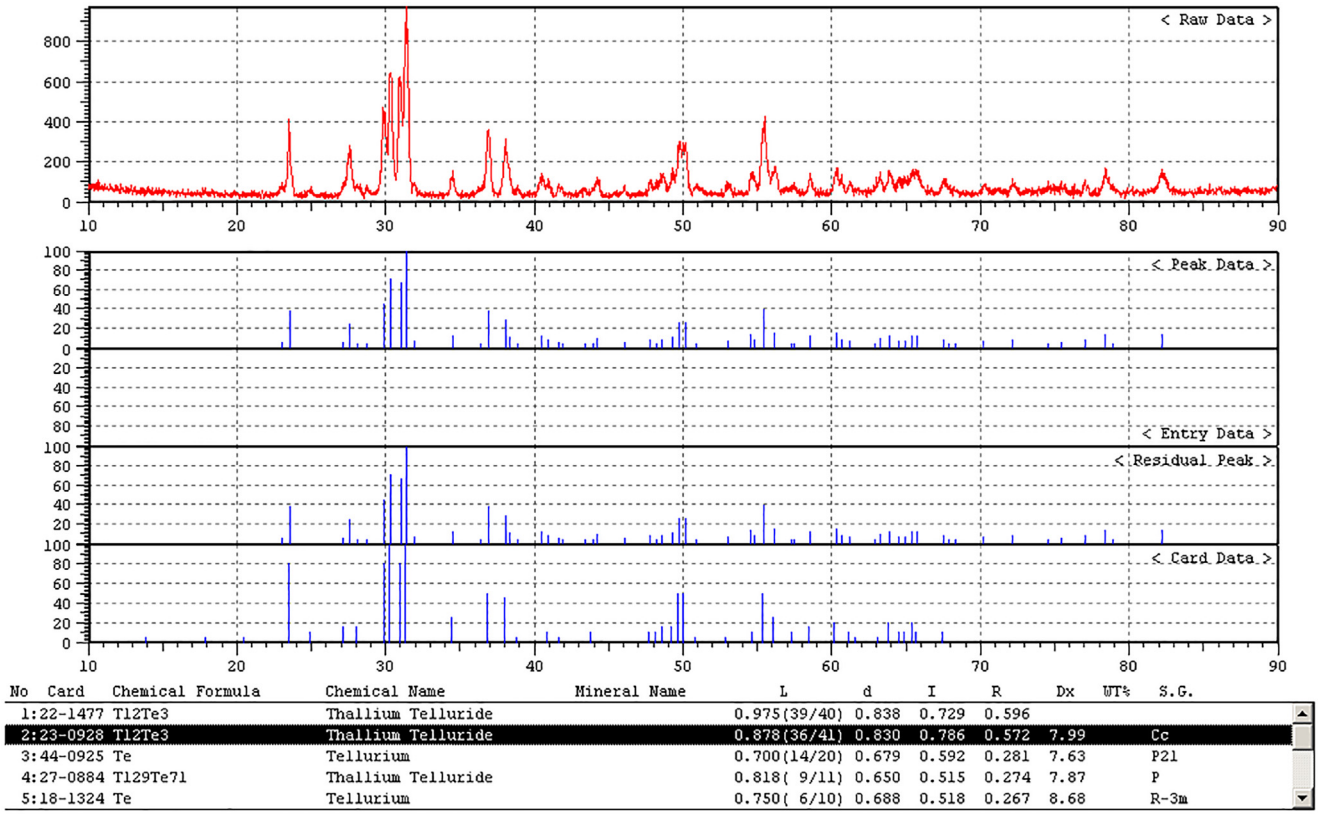

Fig. 1. XRD pattern of Tl2Te3 material and reference patterns of identified components.

curve (6), we can demonstrate the presence of two different kinds modes on mobility variation around the transition temperature i. e 257 K. At low-temperature range $T < 257$ K the mobility behavior increases with the increase of temperature obeying the law $\mu_H \alpha T^{1.86}$, while at low temperatures $\mu_H \alpha T^{-1.7}$. From these results, it seems that the value of the exponent n in the relation $\mu_H \alpha T^n$ is in good agreement with the 1.5 value predicted by theory with those obtained for impurity and lattice scattering in other semiconductors. The room temperature value of the Hall mobility equals 2618 cm^2/V s. The mode of variation of the charge carrier concentration against temperature was checked as a complementary part of the Hall work.

They are calculated by the relation $P = 1/(e R_H)$, which are shown in Fig. 7.

Fig. 7 shows the presence of an ionized acceptor level at 0.103 eV above the top of the valence band obtained is in accordance with that obtained from the conductivity measurements. It can be determined that at room temperature the concentration reaches a value of 1.54×10^{13} cm^{-3}. The variation of the carrier density with temperature appears to be nearly linear, except in the temperature range 173–253 K which represents the region of transition to intrinsic conduction. At low temperature and indeed (93 K–173 K) in Tl_2Te_3, the carrier concentration is determined by the number of ionized acceptors. The figure shows the remarkable increase of carrier concentration in the high-temperature range, where the crystal exhibits an intrinsic behavior. The expected value for the intrinsic concentration can be given as follows [20]:

$$P = 2\left[\frac{2\pi k}{h^2}\right]^{3/2} (m_n^* m_p^*)^{3/4} T^{3/2} \exp\left[\frac{\Delta E_g}{2kT}\right] \quad (4)$$

where m_p^* and m_n^* are the effective mass of holes and electrons, respectively. Using this formula (4), we can calculate the energy gap width of Tl_2Te_3 to be 0.68 eV.

Thermoelectric power (T.E.P) investigation of Tl_2Te_3 single crystals

The thermoelectric power of Tl_2Te_3 single crystals was investigated

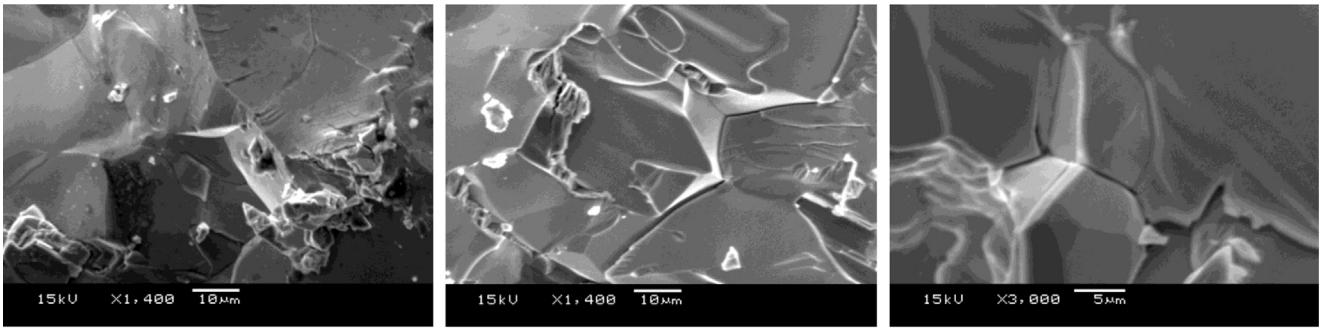

Fig. 2. SEM images of the Tl_2Te_3 single crystals.

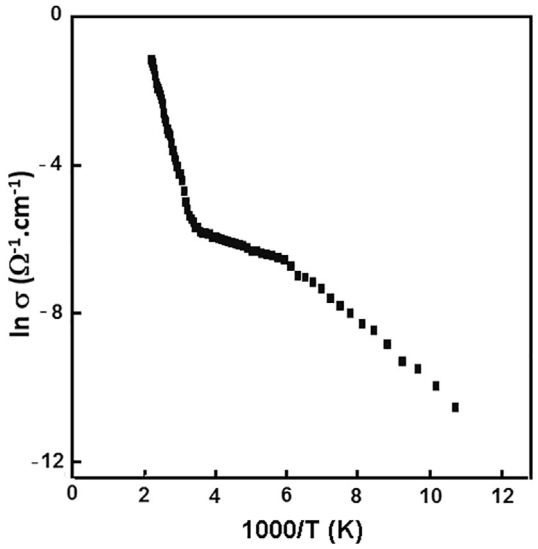

Fig. 3. The temperature dependence of electrical conductivity (σ) for TI_2Te_3 single crystals.

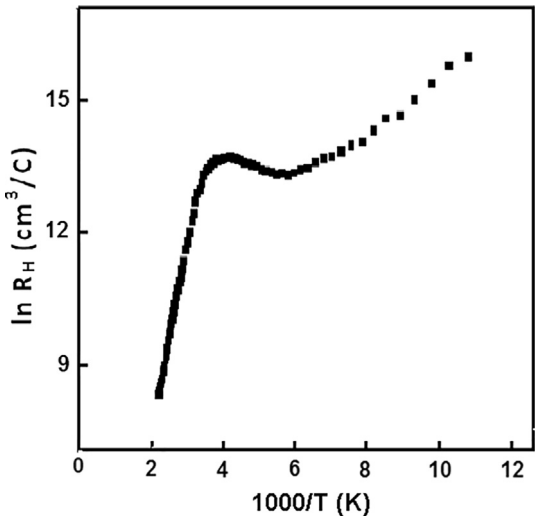

Fig. 4. Hall coefficient (R_H) vs. the temperature for TI_2Te_3 single crystals.

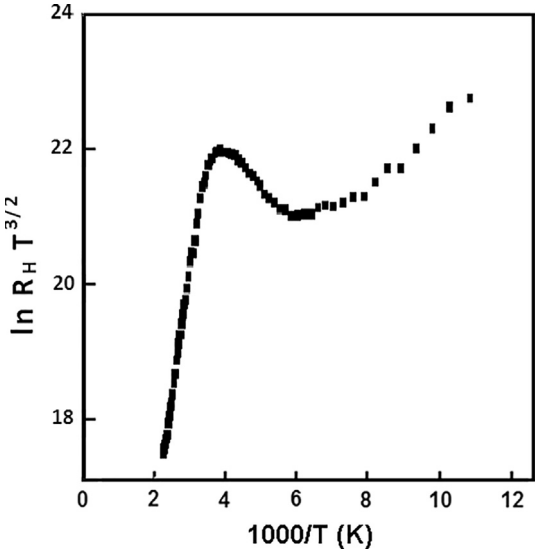

Fig. 5. Temperature dependence of $R_HT^{3/2}$ for TI_2Te_3 single crystals.

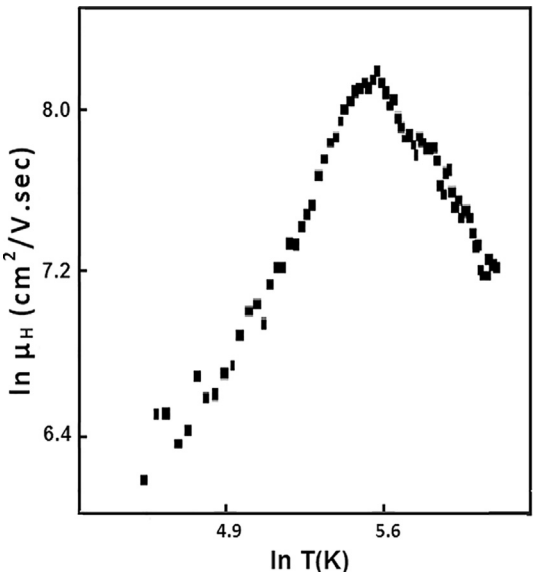

Fig. 6. Temperature dependence of Hall mobility μ_H of TI_2Te_3 single crystals.

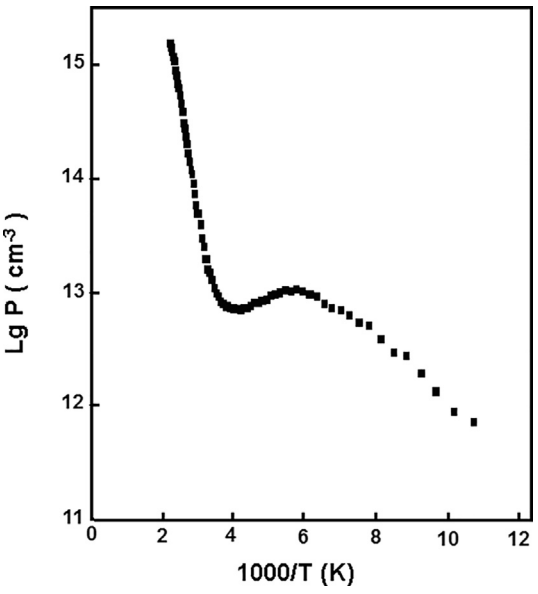

Fig. 7. Dependence of carrier concentration of TI_2Te_3 single crystals on temperature.

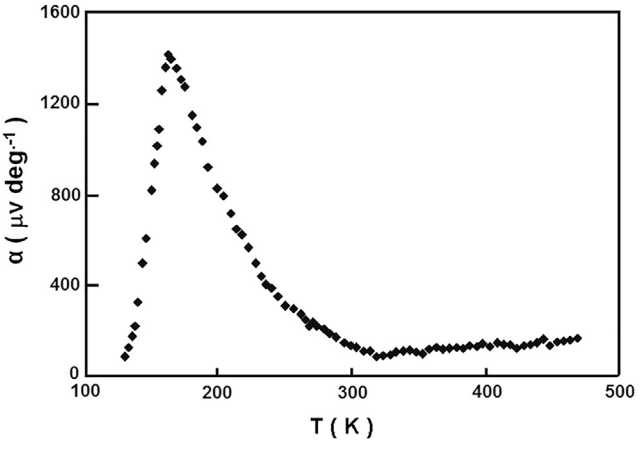

Fig. 8. Temperature dependence of thermoelectric power (α) of TI_2Te_3 single crystals.

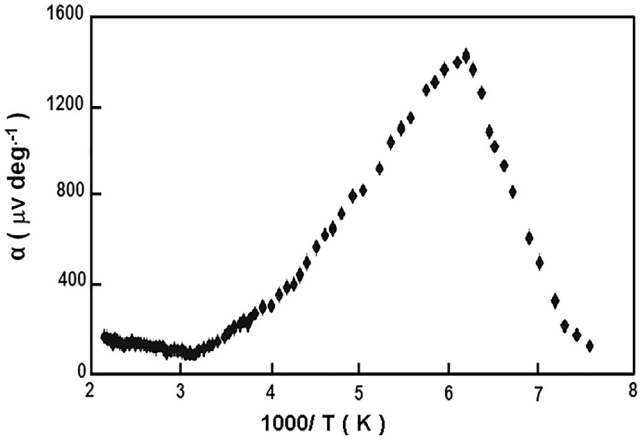

Fig. 9. Thermoelectric power (α) is plotted as a function of reciprocal temperature (1/T) of TI_2Te_3 single crystal.

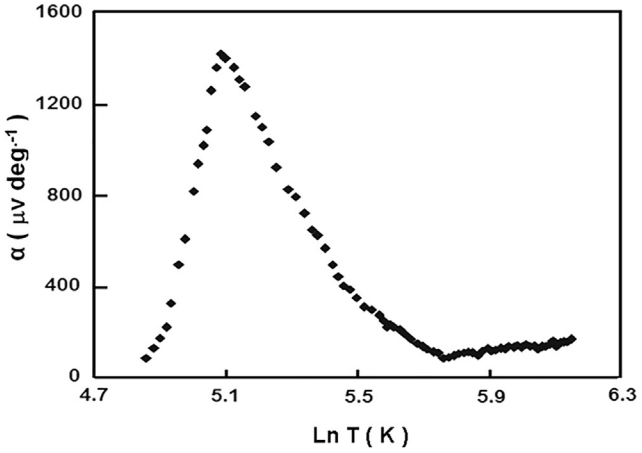

Fig. 10. Variation of the differential thermoelectric power (α) and LnT of TI_2Te_3 single crystals.

in the temperature range from 318 K to 468 K as illustrated in the Fig. 8. The thermoelectric power, (TEP), has been measured for the temperature gradient, ΔT, parallel to the layers plane over a wide temperature range, 129 K–468 K, of the Tl_2Te_3 crystal. It is evident from these measurements that the material has a positive sign throughout the temperature range of investigation. This is in agreement with results obtained from Hall data reported in several works [16,17].

As follows from the behavior of thermoelectric power with temperature in the intrinsic region [21],

$$\alpha = \frac{k}{e}\left[\frac{b-1}{b+1}\left(\frac{\Delta E_g}{2KT}+2\right)\right]-\frac{3}{4}\ln\left(\frac{m_n^*}{m_p^*}\right) \tag{5}$$

Where k is the Boltzmann constant, $b = \frac{\mu_n}{\mu_p}$, μ_n and μ_p are the electron and hole mobility's, and ΔE_g is the energy gap. Eq. (5) predicts that a plot of α against the temperature should be a straight line with parameters determined $b = \mu_n/\mu_p$ and m_n^*/m_p^*. According to this relation, a plot of α vs 1/T would be linear with negative slope, as shown in Fig. 9. The value of $\Delta E_g = 0.69$ eV from Hall data, and assuming that m_n^*/m_p^* does not vary with temperature, we deduce that b = 1.75. Then we can evaluate μ_n and μ_p. Since at room temperature $\mu_p = 2618\ cm^2\ V^{-1}\ s^{-1}$ from Hall measurements, therefore $\mu_n = 4581.5\ cm^2\ V^{-1}\ s^{-1}$. The ratio of electrons and holes effective masses m_n^*/m_p^* is evaluated from the intercept of the curve to be 0.027. It is known that the thermoelectric when one type of carrier dominates is given [22] by:

$$\alpha = \frac{k}{e}\left[2-\ln.\left(\frac{ph^3}{2(2\pi m_p^* KT)^{3/2}}\right)\right] \tag{6}$$

The relation between α and ln T is illustrated in the Fig. 10. This figure indicates that the measured (TEP) increases linearly with the increase of temperature in the temperature range corresponding to extrinsic conductivity region. Fig. 11 depicts carrier-concentration dependence of thermoelectric power (α). We observed a sharp increase in α with the increase of the carrier concentration until carrier density reaches 1420 cm^{-3}, α has a maximum value, with increasing of carrier concentration, α will be decreased sharply until n is equal to $3.357 \times 10^{13}\ cm^{-3}$, Seebeck coefficient (α) increases linearly with increasing carrier concentration.

Fig. 12 shows the Seebeck coefficient (α) versus the logarithm of electrical conductivity (ln σ), according to the relation [23]:

$$\alpha = \frac{k}{e}\left[A+\ln.\left(\frac{2(2\pi m_p^* kT)^{3/2}e\mu}{(2\pi h)^3}\right)\right]-\frac{k}{e}\ln\sigma \tag{7}$$

The behavior of the curve for the relation between electrical

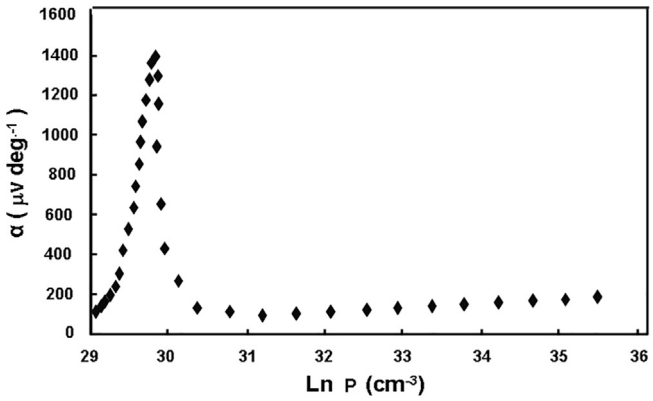

Fig. 11. Differential thermoelectric power dependence of charge carrier concentration for Tl_2Te_3 single crystals.

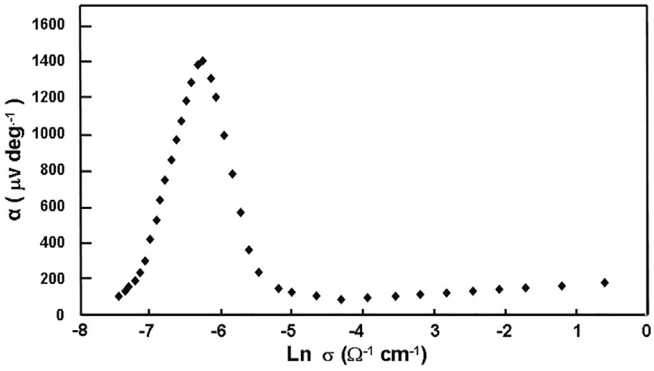

Fig. 12. Variation of the thermoelectric power with electrical conductivity for TI_2Te_3 single crystals.

conductivity and α is similar to that of α versus p.

However, the parameter list of the Tl_2Te_3 single crystals is sufficient to give a complete description.

Conclusion

We have presented Preparation and some physical properties of Tl_2Te_3 Single Crystals. A special new design from melt based on the Bridgman technique has been applied to prepare Tl_2Te_3 single crystals. The crystals were grown with their c-axis perpendicular to the plate-like surface. The grown crystals were characterized by XRD, SEM, EDAX.

The electrical conductivity and Hall effect have been performed over the temperature range from 93 K to 448 K. The temperature range of the thermoelectric power of the studied samples extends from 129 K to 468 K. The crystal was found to have a p-type conductivity throughout the whole range of temperature. Many physical constant have been estimated.

References

[1] Romermann F, Feutelais Y, Fries SG, Blachnik R. Intermetallics 2000;8:53.
[2] Juodakis A, Kannewurf CR. J Appl Phys 1968;39:3003.
[3] Cruceanu E, Sladaru St. J Mater Sci 1969;4:410.
[4] Ikari T, Hashimoto K. Phys. Status Solidi (b) 1978;86:239.
[5] Jensen JD, Burke JR, Ernst DW, Allgaier RS. Phys Rev B 1972;6:319.
[6] Nordell KJ, Miller GJ. J Alloys Compd 1996;241:51.
[7] Lippens PE, Aldon L. Solid State Commun 1998;108:913.
[8] Vassiliev VP, Minaev VS, Batunja LP. Thermodynamic properties phase diagrams and glass-forming of thallium chalcogenides. Chalcogenides Lett 2013;10:485–507.
[9] Rabenau A, Stegherr A, Eckerlin P. Z Metallkde 1960:51–295.
[10] Bhan S, Schubert K. J Less-Common Met 1970;20:229.
[11] Cruceanu E, Slädaru St. J Mater Sci 1969;4(5):410–5.
[12] Shaban HT. Mater Chem Phys 2010;119(1–2):131–4.
[13] Cruceanu E, Sladaru St. J Mater Sci 1969;4:410.
[14] Doert T, Cardoso Gil RH, Böttcher P. The crystal structure of Tl_2Te_3 – a re-investigation. Z Anorg Allg Chem 1999;625:2160–3.
[15] Cruceanu E, Sladaru ST, Boyil T. Phys Status Solidi 1968;30:K149.
[16] Hussein SA, Nassary MM, Gamal GA, Nagat AT. Cryst Res Technol 1993;28(7):1021–6.
[17] Gamal GA, Nassary MM. Cryst Res Technol 1996;31(3):315–21.
[18] Cruceanu E, Sladaru ST, Boyil T. Phys Status Solidi 1968;30:K149.
[19] Langford JI, Wilson AJC. J Appl Cryst 1978;11:102–13.
[20] Dongol M, Nassary MM, Gerges MK, Sebag MA. Turk J Phys 2003;27:211–318.
[21] Lauc J. J Phys Rev 1954;95:1394.
[22] Nassary MM. Turk J Phys 2009;33:201–8.
[23] Schmid PHE, Mooser E. Helv Phys Acta 1972;45:870.